

Research Paper

## Effect of Fluoride Coating on the Degradation of Mg-Based Alloy Containing Calcium for Biomedical Applications

**Abouzar Rezaei-Baravati, Masoud Kasiri-Asgarani\*, Hamid Reza Bakhsheshi-Rad†, Mahdi Omid, Ebrahim Karamian**

*Advanced Materials Research Center, Department of Materials Engineering, Najafabad Branch, Islamic Azad University, Najafabad, Iran*

---

### ARTICLE INFO

#### *Article history:*

Received 27 October 2021  
Accepted 29 December 2021  
Available online 1 January 2022

#### *Keywords:*

*Magnesium alloy  
Corrosion behavior  
Fluoride treatment  
Surface treatment  
Weight loss*

---

### ABSTRACT

The effect of hydrofluoric acid (HF) treatment on the corrosion performance of the Mg–Zn–Al–0.5Ca alloy was studied by immersing a specimen in HF solutions for varying lengths of time at room temperature. X-ray diffraction (XRD), scanning electron microscopy (SEM), and atomic force microscopy (AFM) were used to study the evolution of microstructures. In vitro corrosion resistance was assessed using potentiodynamic polarization and a room-temperature immersion test in simulated body fluid (SBF). The fluoride-treated Mg–Zn–Al–0.5Ca alloy formed by 24h immersion in HF exhibited a more homogeneous, compact, and thicker (2.1 μm) coating layer compared to the other HF treated specimens in 6, 12, and 18 hours. The corrosion resistance performance of the Mg–Zn–Al–0.5Ca alloy formed by 24h immersion in HF was the best, with a corrosion rate of 2.87 mm/y according to the electrochemical experiment. The mean weight loss of the untreated samples was considerably higher (up to 2 times) than that of the fluoride-treated alloys, according to in vitro degradation assessments. According to the findings, the fluoride-treated Mg–Zn–Al–0.5Ca alloy is a promising candidate for biodegradable implants because of its low degradation kinetics and apatite formation ability.

---

**Citation:** Rezaei-Baravati, A.; Kasiri-Asgarani, M.; Bakhsheshi-Rad, H.R.; Omid, M.; Karamian, E. (2022) Effect of Fluoride Coating on the Degradation of Mg-Based Alloy Containing Calcium for Biomedical Applications, Journal of Advanced Materials and Processing, 10 (1), 67-76. Dor: 20.1001.1.2322388.2022.10.1.6.9

#### **Copyrights:**

Copyright for this article is retained by the author (s), with publication rights granted to Journal of Advanced Materials and Processing. This is an open – access article distributed under the terms of the Creative Commons Attribution License (<http://creativecommons.org/licenses/by/4.0>), which permits unrestricted use, distribution and reproduction in any medium, provided the original work is properly cited.



---

† **Corresponding Authors**

E-mail Address: m.kasiri@pmt.iaun.ac.ir; rezabakhsheshi@pmt.iaun.ac.ir

## 1. Introduction

Mg and its alloys have been extensively investigated as biodegradation implant materials due to their remarkable qualities, such as analogous density (1.74–1.84 g/cm<sup>3</sup>) and elastic modulus (41–45 GPa) to human bones, high strength to weight ratio, and good biocompatibility. Nevertheless, the high corrosion rate and localized/pitting corrosion behavior reduced their mechanical solidity as an implant, severely restricting magnesium alloy's therapeutic application for orthopedic fixation systems [1]. Presently, the corrosion rate of magnesium can be controlled by employing two methodologies: composition alteration and alloy surface treatment. One of the essential tools for enhancing the corrosion resistance of Mg alloy is alloying. Ca is an essential alloying component in human bone, and the release of Mg and Ca ions can improve bone recovery [2]. Zinc can also enhance castability, increase age-hardening response, form intermetallic compositions, alter and refine grain size. The incorporation of aluminum improves fluidity and tensile strength by strengthening the solid solution and corrosion resistance [3]. Aluminum at low concentrations has been proposed as an alloying element for biomedical applications. Surface modification, in addition to micro-alloying, is used to boost the corrosion resistance of magnesium alloys. For medical applications, the ideal magnesium alloy coating has characteristics such as corrosion resistance, degradability, and biocompatibility [4]. Surface modifications are classified based on the approach of coating preparation, which includes mechanical, physical, chemical, and biological or biomimetic [5-7]. The reaction between the magnesium substrate and the conversion coated media produces a chemical coating layer that is strongly bonded to the substrate. Because it is based on chemical reactions, it might be more susceptible to thermodynamics and kinetics [4]. Recently, fluoride treatment has been considered to be an effective method for preparing a protective chemical fluoride conversion coating (MgF<sub>2</sub>) for Mg alloy with high corrosion resistance [8]. Fluoride coatings have been shown to improve the corrosion resistance of magnesium alloys [9, 10] and to have proper biocompatibility. Furthermore, it is assumed that the film has a high binding force with the magnesium matrix attributed to the presence of chemical bonds between magnesium and fluoride ions [11]. The coating layer (MgF<sub>2</sub>) has also been indicated to present high density while staying chemically inert and nontoxic, as well as lowering solubility in water. Furthermore, fluorine is a component of human bone and teeth [12]. In this study, fluoride coating was generated on Mg–Zn–Al–0.5Ca alloy, and its compositions, microstructures,

electrochemical, and in vitro dynamic degradation performance were investigated.

## 2. Materials and methods

### 2.1. Specimen preparation

Pure Mg ingot (99.9%), high purity Al chips (99.9%), pure zinc chips (99.9%), and Mg–40Ca master alloy were used as starting materials. In a mild steel crucible with argon gas flow, the components were melted for 30 minutes at 690°C. Upon the melting and alloying procedures, molten metal with a 0.5 weight percent Ca concentration was poured into a pre-heated mild steel mold to form ingots. Several disk samples (φ15mm × 5mm) were cut from the ingots. Each specimen's surface was wet-ground with 320 to 2000 silicon carbide emery papers before rinsing twice in distilled water. And after electro-polishing at room temperature was microstructurally analyzed using scanning electron microscopy.

### 2.2. Conversion coating treatment and characterization

A warm air flow was utilized to dry the polished specimens after being bathed entirely with distilled water, rinsed, and degreased ultrasonically with ethanol. Finally, the specimens were bathed with distilled water, dried, and stored for future inquiry. After that, the specimens were immersed in 40 wt.% hydrofluoric acid at room temperature for varying lengths of time (6, 12, 18, and 24 h). After being treated with hydrofluoric acid, the samples were rinsed with distilled water and air-dried. The samples before any treatment and the final mass after each period of immersion were measured using analytic balance to evaluate the mass change. The microstructures of the untreated and fluoride-coated specimens were confirmed by scanning electron microscopy (SEM, Jeol Jsm-6380LA), and the chemical compound of the alloys was determined by energy-dispersive spectroscopy (EDS, Zeiss Supra 33VP). The microstructural stages of the untreated and treated specimens were determined using X-ray diffractometry (XRD). The experiment was conducted using a diffractometer (XRD, Siemens D500) using Cu–K<sub>α</sub> ( $\lambda = 1.540598 \text{ \AA}$ ) radiation and operated at 40 kV and 35 mA. The specimens' surface topography was examined utilizing an atomic force microscope (AFM, NanoScope IV, Digital Equipment) (tapping). A non-contact microscope was used to capture the images.

### 2.3 Corrosion test

#### 2.3.1 Electrochemical tests

The electrochemical test was conducted in a glass cell that includes 200 mL of Kokubo simulated body fluid (SBF) [13] at pH 7.66, utilizing Versastat 3 potentiostat/ galvanostat (Princeton Applied Research) at 37 °C. Table 1 shows the chemical combination of the SBF medium. Furthermore, for

the potentiodynamic polarization assessments, a saturated calomel electrode (SCE) and a graphite rod were utilized as the reference and counter electrodes, respectively, with the sample serving as the working electrode in a three-electrode cell. All tests were recorded at a scan rate of 0.5 mV/s, beginning at  $-250$  mV<sub>SCE</sub> below the open circuit potential. The specimens' surfaces were exposed to the solution. The exposed area surface was approximately 1 cm<sup>2</sup>.

For each treatment condition, four measurements were carried out as well for the untreated specimens. This fitting can be controlled manually using the software. A section of the curve from  $E_{\text{corr}}$  (V<sub>SCE</sub>) was selected for the Tafel fittings, and  $i_{\text{corr}}$  was determined from the value where the fit met the  $E_{\text{corr}}$  (V<sub>SCE</sub>) potential value. All testing was conducted three times to confirm the reproducibility of the findings.

**Table 1.** Kokubo simulated body fluid's chemical compound.

Solution	Ion concentration (mmol/L)							
	Na <sup>+</sup>	K <sup>+</sup>	Ca <sup>2+</sup>	Mg <sup>2+</sup>	HCO <sub>3</sub> <sup>-</sup>	Cl <sup>-</sup>	HPO <sub>4</sub> <sup>2-</sup>	SO <sub>4</sub> <sup>2-</sup>
Human blood plasma	142.0	5.0	2.5	1.5	27.0	103.0	1.0	0.5
Kokubo (c-SBF)	142.0	5.0	2.5	1.5	4.2	147.8	1.0	0.5

### 2.3.2 Immersion test

For in vitro testing, fluoride-coated and untreated specimens were immersed in 150 mL Kokubo simulated body fluid (SBF) at pH 7.66, according to ASTM G31-72. The beakers were sealed and incubated at a consistent temperature of 37 °C for a week. Following that, the specimens were extracted from the SBF, gently washed with distilled water, and dried in room temperature air for surface examination. To determine the average corrosion rate, specimens were immersed in acetone, deionized water solution for varying lengths of time and then cleaned in acetone, and deionized water solution to remove corrosion products developed on the specimens. The corrosion rate was calculated as follows:

$$C_R = \frac{W}{A \rho t} \quad (1)$$

where  $C_R$  indicates corrosion rate and  $w$  represents weight loss  $A$  is the initial surface area exposed to SBF;  $\rho$  is the density of Mg alloy; while  $t$  is the length of immersion employed in this investigation [12]. SBF specimens were immersed for 12 h intervals. The average pH of the samples was taken from three measurements. After the immersion test, the surface appearance of corroded specimens was looked at by using SEM and EDS to look at them.

## 3. Results and discussion

### 3.1 Preparation of specimens

In a displacement reaction, magnesium and HF form MgF<sub>2</sub> layer, which is insoluble and provides a barrier

coating for magnesium. Initial studies with MZA-0.5Ca samples in HF at varied treatment periods demonstrated a quite slow reaction between Mg and HF. There were few or no bubbles noticed during immersion. The time change of the increase in mass per unit area is seen in Fig.1. With increasing immersion time, the graph reveals a constant rise in mass and thus growth of the MgF<sub>2</sub> film, although the rate of progress is slow. It is worth noting that slow growth of MgF<sub>2</sub> film due to its character as a barrier. Nevertheless, the increase in mass must only be described as an estimate of the MgF<sub>2</sub> film growth. A simple conversion of mass added to film thickness taking an increase from F would result in an underrate. This is due to the dissolution of Mg into the acid and removing the oxide/hydroxide from the sample surface, which would lower the mass. As the immersion time for all samples increased from 18 to 24 h, the slope of the mass curve, as shown in Fig. 1, decreased due to a decrease in deposition rate. These results were similar to prior investigations, which indicated that deposit development might occur at the film/metal interface since the mobility of the F ions is high. As a result, as the film thickness grows, deposit growth decreases.

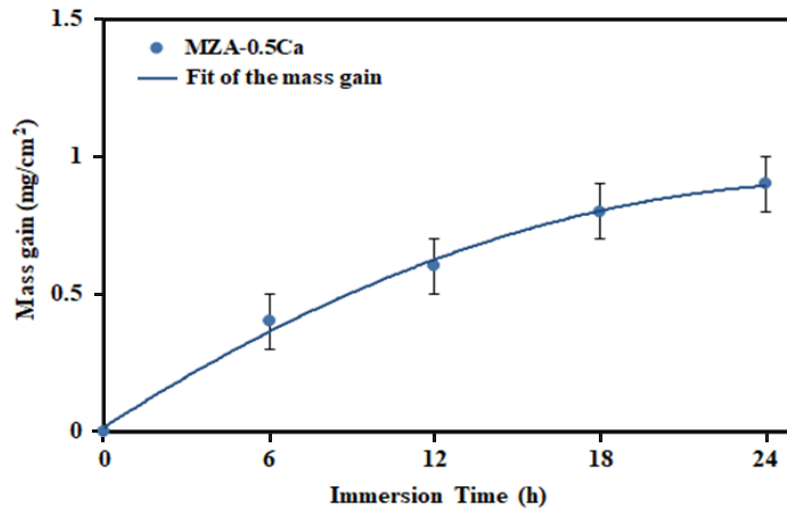


Fig. 1. Variation of specific mass gain of sample as a function of HF treatment time.

As shown in Fig. 2, the appearance of the specimens altered dramatically with treatment time. With immersion times of 6, 12, 18, and 24 h, the specimens were light-bronze, dark-bronze, light-golden, dark-golden, and black. The specimens had a grey color

after 24 h of immersion, which darkened with increasing treatment time, eventually resulting in black color. This variation in the specimens suggests the existence of various compounds on the sample surface.

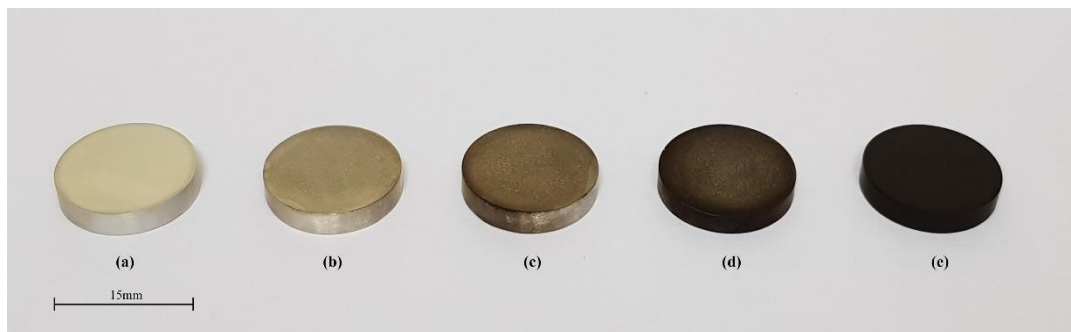


Fig. 2. Optical images of (a) untreated sample, and samples after immersion in the 40% HF solution for (b) 6 h, (c) 12 h, (d) 18 h and (e) 24 h.

### 3.2 Microstructure and coating characterization

The microstructure of untreated MZA–0.5Ca alloy is shown in Fig. 3a to be composed of  $\alpha$ -Mg matrix,  $Mg_{17}Al_{12}$ , and  $(Mg,Al)_2Ca$  phases.  $Mg_{17}Al_{12}$  precipitates with spherical morphology were found inside the equiaxial grains of  $\alpha$ -solid solution, according to microstructure analyses. Phase  $(Mg,Al)_2Ca$  has been identified using XRD and EDS analysis, with some Al entering the  $Mg_2Ca$  structure. Based on the Mg–Ca and Mg–Al–Ca phase diagrams, a small content of calcium can be dissolved in the  $\alpha$ -Mg matrix, so it is possible that the lamellar eutectic  $(Mg,Al)_2Ca$  particles form during melt solidification and the tiny granular  $(Mg,Al)_2Ca$  particles form after solidification. Fig. 3b–e illustrates the surface morphology of fluoride-treated samples following the immersion in HF acid for 24 hours. On the surface of the specimen, a compact film with some irregularly distributed pores can be seen. Many corrosive micro-batteries could be created on the

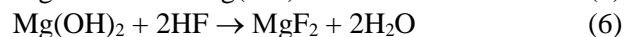
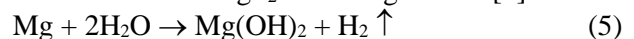
surface of the specimen when they were immersed in hydrofluoric acid. The magnesium might be dissolved in the micro-anode region [9] and reactions could occur as follows:



Meanwhile, the  $Mg^{2+}$  reacted with  $F^-$  ion, and thus  $MgF_2$  can be established and reactions could occur as follows [9]:



As the reaction progresses, the reaction interface of magnesium dissolution should be reduced, and thus the deposition of  $MgF_2$  should be slowed. As a result, as the thickness of the film increased, its growth slowed. After 24 h of immersion in hydrofluoric acid, the surface barrier film was thick enough just to stop the reaction. An oxidation reaction occurred during the formation of  $MgF_2$  according to Ref. [9]:



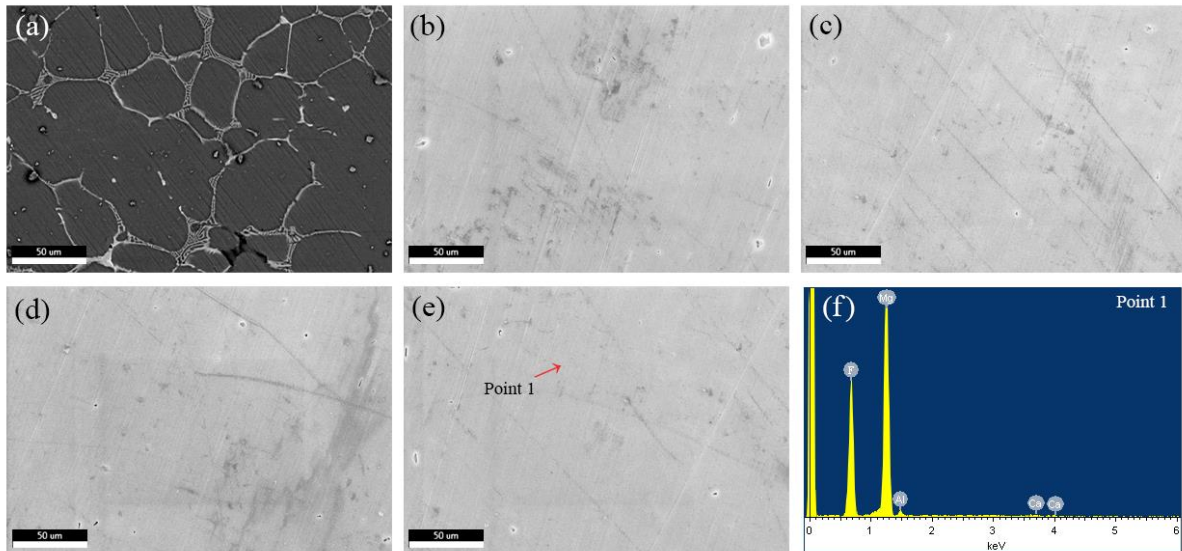


**Fig. 3.** SEM images of the (a) untreated sample, and fluoride-coated MZA-0.5Ca samples after immersion in the 40% HF solution for (b) 6 h, (c) 12 h, (d) 18 h, (e) 24 h, and (f) EDS spectrum of point 1.

The coating layer is composed of Mg, Ca, Al and F elements, according to EDS analysis of treated samples (Fig. 3f). The presence of fluoride demonstrated that HF acid was involved in creating the coating layer. Since the coating was narrow, the alloy substrate was also recognized in the range with excellent resolution [9, 14]. Furthermore, the XRD patterns of the untreated sample are shown in Fig. 4a, where low intensities peaks related to the  $Mg_{17}Al_{12}$  and  $(Mg,Al)_2Ca$  phases were observed in the MZA-0.5Ca alloy [15]. During the primary processing of this alloy, the presence of such particles may cause the development of specific dynamic and static recrystallization behaviors [16]. The XRD pattern from the fluoride conversion layer on MZA-0.5Ca

alloy is shown in Fig. 4. Aside from the peaks of  $\alpha$ -Mg substrates, some new peaks were detected due to  $MgF_2$  reflection. According to the XRD results, the film on the MZA-0.5Ca alloy is  $MgF_2$ . The low intensity of the diffraction peaks implies that  $MgF_2$  has low crystallinity.

Fig. 5 clearly shows that the thickness of the fluoride conversion coating was proportional to the treatment time. With increasing treatment time, the fitting curve shows a monotonic increase in thickness and thus growth of the fluoride coating. However, as the treatment continued, the rate of growth slowed. The coating thickness had achieved a constant value of about 2.1  $\mu m$  after 24 h.

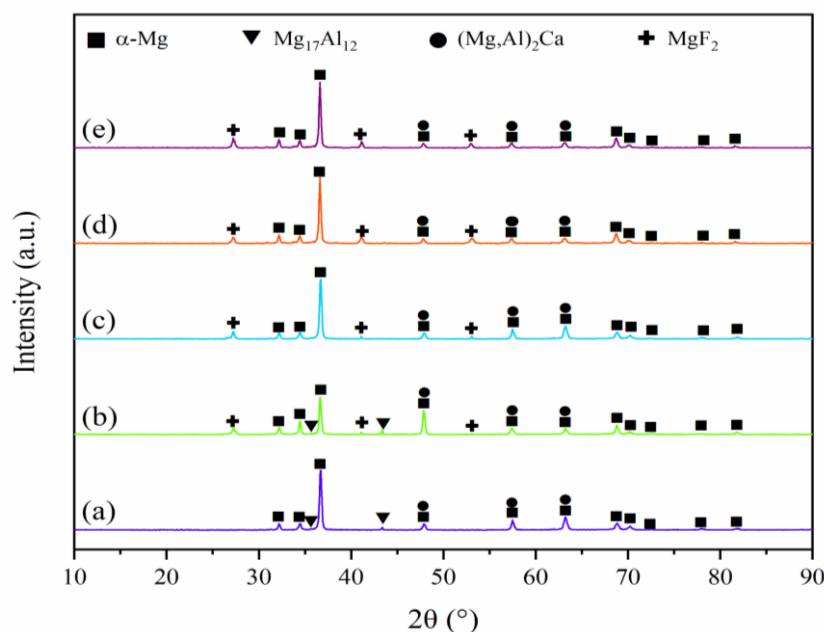


**Fig. 4.** XRD patterns of (a) untreated sample, and fluoride-coated MZA-0.5Ca samples after immersion in the 40% HF solution for (b) 6 h, (c) 12 h, (d) 18 h and (e) 24 h



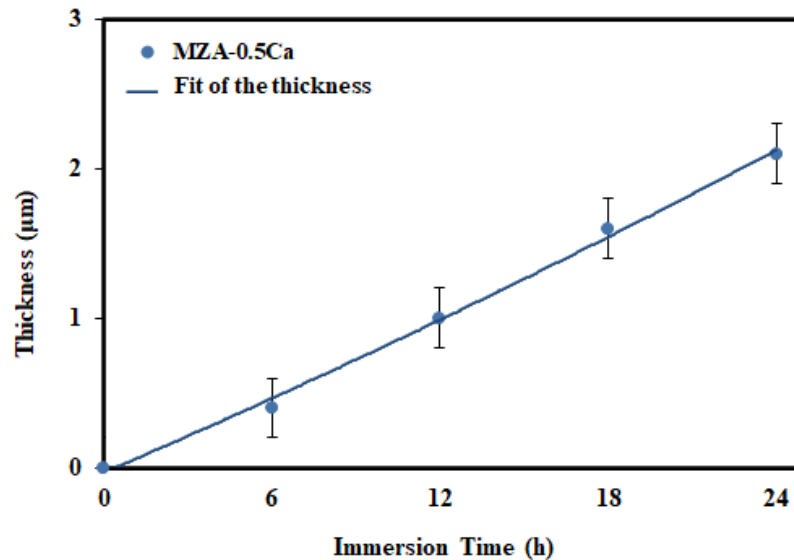


Fig. 5. Variation of coating thickness on MZA-0.5Ca as a function of HF treatment time

Fig. 6 depicts the mean surface roughnesses ( $R_a$ ) of treated and untreated specimens. The corrosion behavior of the treated samples is significantly influenced by surface roughness. It was demonstrated that decreasing sample surface roughness reduced surface area for the corrosive attack [17]. The surface

may become coarser after fluoride treatments, according to atomic force microscope (AFM) measurements. Untreated specimens had an average roughness of 271 nm, while 24h treated specimens had an average roughness of 335 nm.

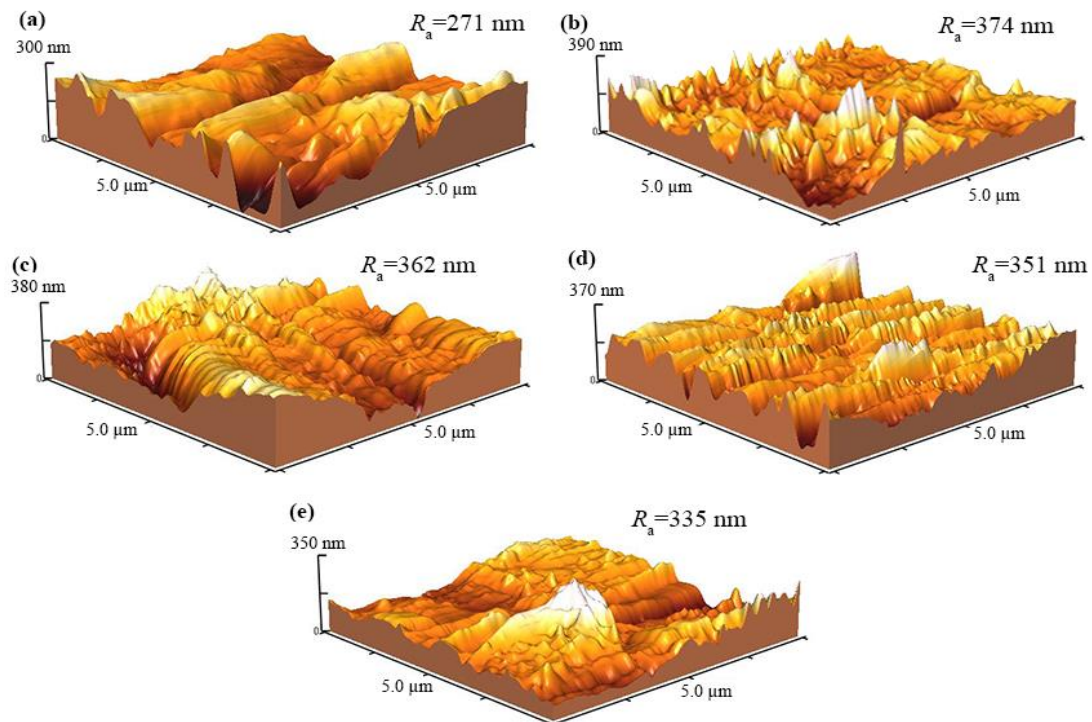


Fig. 6. Atomic force microscopy of (a) untreated specimens and fluoride-coated MZA-0.5Ca specimens following the immersion in a 40% HF solution for (b) 6 h, (c) 12 h, (d) 18 h, and (e) 24 h.

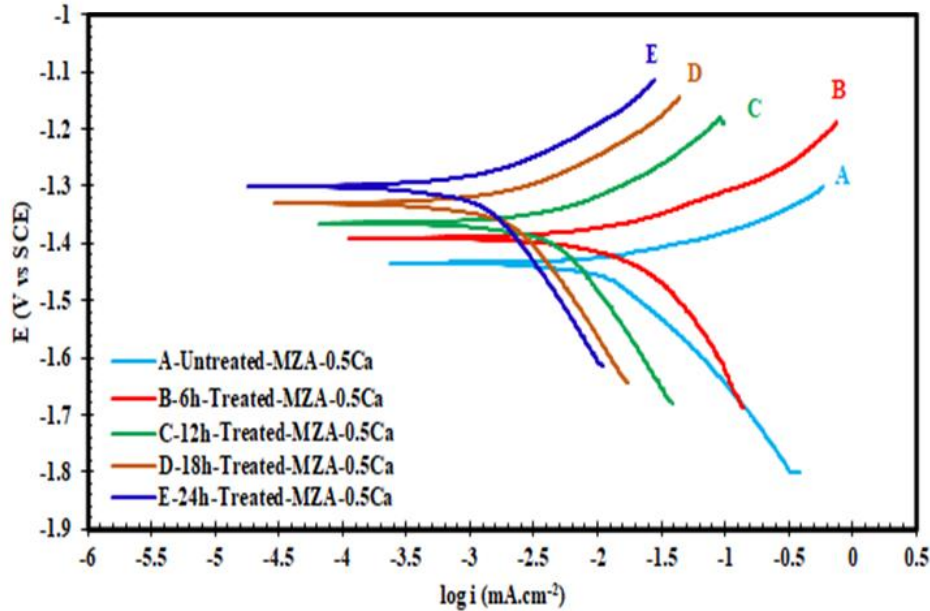
### 3.3 Electrochemical measurement

Fig. 7 depicts typical polarization curves in Kokubo solution for untreated and treated samples. Table 2 shows the corrosion potential  $E_{corr}$  and corrosion current density  $i_{corr}$  values derived from these curves. The  $E_{corr}$  was ennobled due to the fluoride layer, which functioned as a barrier. After 24 h of

immersion in hydrofluoric acid, the corrosion rate was reduced to 2.87 mm/year. The polarization curve approximately corresponded in time with that of the untreated sample. Increased immersion duration in the HF solution would raise specimen corrosion resistance ultimately. The corrosion rate of specimens treated for 6, 12, and 18 hours, is higher

than that of those treated for 24 hours. Corrosion resistance is reduced due to cracks in the coating.  $\text{Cl}^-$  ions might enter the cracks and come into touch with the Magnesium substrate. The cathodic current, which exhibits hydrogen evolution, declined with a lower slope in the treated samples than in untreated samples when the applied potential increased. As the applied potential increased, the anodic current, which

shows specimen dissolution, increased with a greater slope in the untreated specimen than in the coated specimens. This behavior might be caused by localized corrosion and then the pit growth [18]. The corrosion potential has been shifted slightly to the negative side. Even a very thin film of  $\text{MgF}_2$  appears to be sufficient to significantly slow down corrosion.



**Fig. 7.** Polarization curves for untreated MZA-0.5 and fluoride-coated MZA-0.5 samples in SBF solution at 37 °C.

**Table 2.** Parameters obtained from polarization curves for untreated MZA-0.5 and fluoride-coated MZA-0.5 samples in SBF solution at 37 °C

Specimen	$E_{corr}$ (mV vs. SCE)	$i_{corr}$ ( $\mu\text{A}/\text{cm}^2$ )	Corrosion rate, $C_R$ (mm/year)
Untreated-MZA-0.5Ca	$-1435 \pm 12$	$162 \pm 13$	$3.7 \pm 0.21$
6h-Treated-MZA-0.5Ca	$-1389 \pm 11$	$153 \pm 14$	$3.49 \pm 0.28$
12h-Treated-MZA-0.5Ca	$-1372 \pm 15$	$144 \pm 15$	$3.29 \pm 0.25$
18h-Treated-MZA-0.5Ca	$-1341 \pm 14$	$135 \pm 12$	$3.08 \pm 0.24$
24h-Treated-MZA-0.5Ca	$-1309 \pm 11$	$126 \pm 13$	$2.87 \pm 0.22$

### 3.4 In vitro degradation mechanism of fluoride coated MZA-0.5Ca alloy

Fig. 8 depicts the weight loss of untreated and fluoride-treated (40% HF treated) samples in Kokubo solution after 168 hours. During the initial stages of the test, it was discovered that the film might operate as a corrosion barrier covering the matrix, leading to a much-reduced degradation rate of the treated specimens in comparison with the untreated specimens. The degradation rate of fluoride-treated samples is influenced by two factors. The thickness of the coating layer is the first consideration. It was

discovered during chloride solution testing that increasing the thickness of the dense layer inhibits the additional corrosion in Mg [19]. Surface roughness is another element that influences the corrosion rate of treated samples. Nevertheless, the weight loss rate was dramatically decreased after 72 hours due to the deposition of hydroxyapatite (HAp) on the sample [20]. For the entire stage, treated specimens had significantly lower mass losses than untreated specimens. This indicated that the  $\text{MgF}_2$  film might operate like a corrosion-barrier covering on the alloy, resulting in a decreased degradation rate on the MZA-0.5Ca alloy.

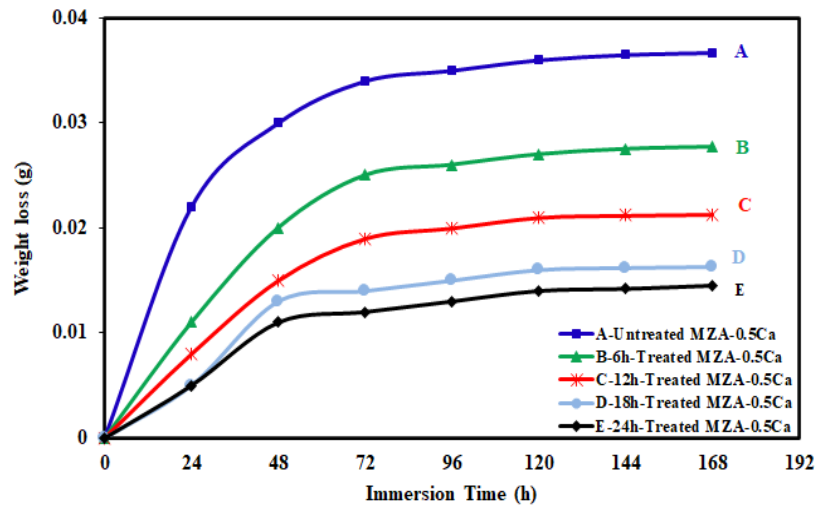


**Fig. 8.** The weight loss of untreated MZA-0.5 and fluoride-coated MZA-0.5 samples as a function of immersion time in SBF solution

### 3.5 Immersion tests

Fig. 9a depicts the variation in pH value and the volume of hydrogen evolution of uncoated and fluoride-coated MZA-0.5 samples as a function of the immersion time in SBF solution. The  $MgF_2$  coating also protected the treated alloys from fast degrading

when the pH of the immersion solution was increased slightly. The hydrogen evolution volume of treated and untreated samples had an almost linear relationship with immersion duration, which can be seen in Fig. 9b; where untreated alloys generated much more hydrogen bubbles than  $MgF_2$ -coated alloys.

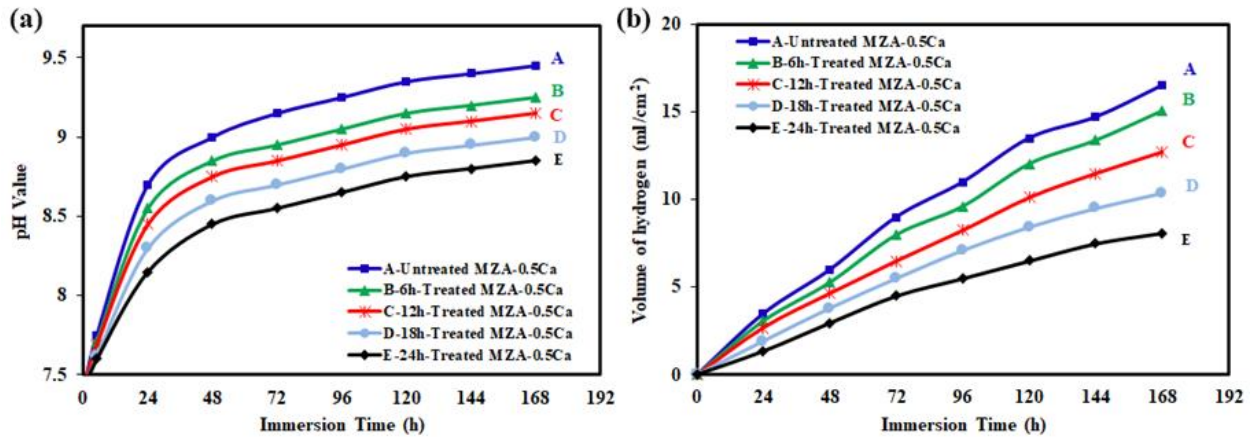


**Fig. 9.** (a) The variation in pH value in SBF solution and (b) the hydrogen evolution volume of uncoated and fluoride-coated MZA-0.5 samples as a function of the immersion time in SBF solution.

The surface morphology of the untreated and treated MZA-0.5Ca alloys after 168 h in SBF solution is shown in Fig. 10. Untreated samples were found to have a severe corrosion attack as shown in Fig. 10 (a,b). The EDS analysis in Fig. 10 shows that the corroded sample surface contained C, O, P and primarily Mg, with trace Ca detected. The surface morphology of the samples ( $MgF_2$ -coated) after 6, 12, 18, 24h HF-treatment for 168 h immersion are shown in Fig. 10(c-j). After the immersion test, the surface of the HF-treated sample experienced mild

corrosion attacks, while untreated samples suffered from serious corrosion attacks. The  $MgF_2$  coating shields the treated samples from the electrolyte, reducing chloride ion corrosive attack. As a result, corrosion of treated samples cannot begin until the protective coating has dissolved or peeled. The reduction of corrosion rate of Mg alloy implants is guaranteed by the service life of the surface coating [21,22]. The EDS analysis shows that compounds rich in Ca and P had deposited on the  $MgF_2$  film which may imply the formation of hydroxyapatite.



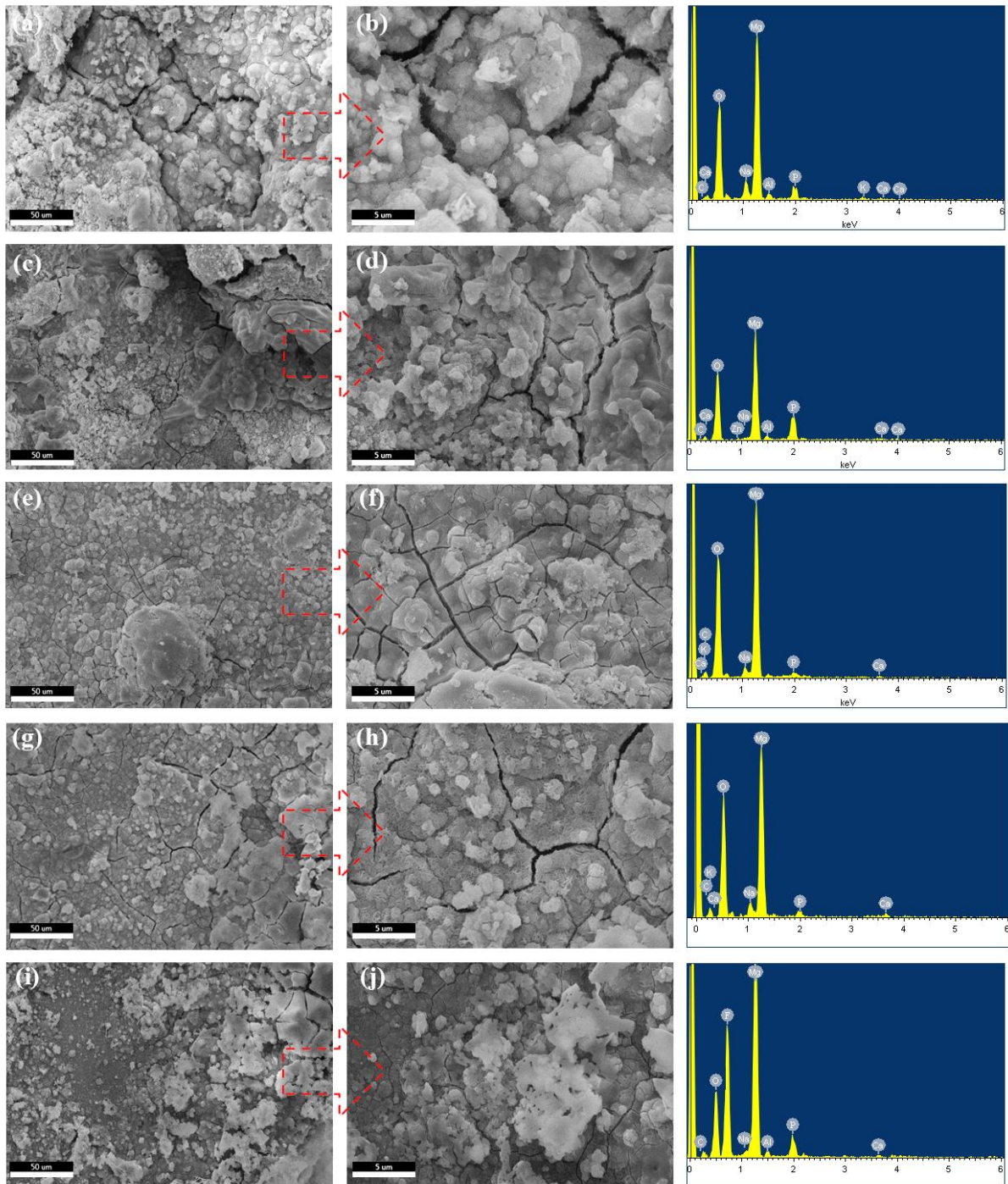


**Fig. 10.** The surface morphologies and EDS spectrum of (a,b) uncoated MZA-0.5Ca alloy, and samples after (c,d) 6h, (e,f) 12h, (g,h) 18h and (i,j) 24h F-treatment for 168 h immersion in SBF solution and corresponding EDS analysis.

#### 4. Conclusions

On the MZA-0.5Ca alloy, a facile conversion coating method was established employing HF at room temperature. The corrosion resistance in SBF solution was tested after the coated specimens were characterized and the following conclusions were attained.

1) A uniform and compact coating of about  $2.1 \mu\text{m}$  thick was created after 24 hours of immersion in 40% HF, and the conversion immersion was mainly composed of tetragonal  $\text{MgF}_2$ .

2) EIS and polarization tests exhibited that the fluoride conversion coating significantly increased corrosion resistance. In addition, the degradation rate in vitro of fluoride-treated alloys in the SBF solution is slower than the untreated alloys.

3) A viable option for biodegradable medical implants is MZA-0.5Ca alloy treated with HF for 24 hours because of its low degradation kinetics and formation of corrosion protective layers on the surface of MZA-0.5Ca alloy.

## References

- [1] C. Zhang, S. Zhang, D. Sun, J. Lin, F. Meng, H. Liu, "Superhydrophobic fluoride conversion coating on bioresorbable magnesium alloy—fabrication, characterization, degradation and cytocompatibility with bmscs", *J. Magnesium Alloys*, Vol. 9, No. 4, 2021, pp. 1246-1260.
- [2] S. Ghaedi Faramoushjadi, F. Chinaei, H.R. Bakhsheshi-Rad, M. Hasbullah Idris, "Effect of fluoride conversion coating on corrosion behavior of mg-ca-zn alloy", *Proc. Advanced Materials Research*, 2013, pp. 3-6.
- [3] I. Baghni, Y.-S. Wu, J.-Q. Li, C. Du, W. Zhang, "Mechanical properties and potential applications of magnesium alloys", *Trans. Nonferrous Met. Soc. China*, Vol. 13, No. 6, 2003, pp. 1253-1259.
- [4] Z.-Z. Yin, W.-C. Qi, R.-C. Zeng, X.-B. Chen, C.-D. Gu, S.-K. Guan, Y.-F. Zheng, "Advances in coatings on biodegradable magnesium alloys", *J. Magnesium Alloys*, Vol. 8, No. 1, 2020, pp. 42-65.
- [5] X. Xiong, Y. Yang, J. Li, M. Li, J. Peng, C. Wen, X. Peng, "Research on the microstructure and properties of a multi-pass friction stir processed 6061al coating for AZ31 Mg alloy", *J. Magnesium Alloys*, Vol. 7, No. 4, 2019, pp. 696-706.
- [6] Y. Guo, Y. Zhang, Z. Li, S. Wei, T. Zhang, L. Yang, S. Liu, "Microstructure and properties of in-situ synthesized ZrC-Al3Zr reinforced composite coating on AZ91D magnesium alloy by laser cladding", *Surf. Coat. Technol.*, Vol. 334, 2018, pp. 471-478.
- [7] X.-B. Chen, H.-Y. Yang, T.B. Abbott, M.A. Easton, N. Birbilis, "Corrosion protection of magnesium and its alloys by metal phosphate conversion coatings", *Surf. Eng.*, Vol. 30, No. 12, 2014, pp. 871-879.
- [8] S. Li, L. Yi, X. Zhu, T. Liu, "Ultrasonic treatment induced fluoride conversion coating without pores for high corrosion resistance of Mg alloy", *Coatings*, Vol. 10, No. 10, 2020, pp. 996.
- [9] T. Yan, L. Tan, D. Xiong, X. Liu, B. Zhang, K. Yang, "Fluoride treatment and in vitro corrosion behavior of an AZ31B magnesium alloy", *Mater. Sci. Eng., C*, Vol. 30, No. 5, 2010, pp. 740-748.
- [10] F. Witte, J. Fischer, J. Nellesen, C. Vogt, J. Vogt, T. Donath, F. Beckmann, "In vivo corrosion and corrosion protection of magnesium alloy LAE442", *Acta Biomater.*, Vol. 6, No. 5, 2010, pp. 1792-1799.
- [11] Y. Chen, Y. Song, S. Zhang, J. Li, H. Wang, C. Zhao, X. Zhang, "Effect of fluoride coating on in vitro dynamic degradation of Mg–Zn alloy", *Mater. Lett.*, Vol. 65, No. 17-18, 2011, pp. 2568-2571.
- [12] M. Ren, S. Cai, T. Liu, K. Huang, X. Wang, H. Zhao, S. Niu, R. Zhang, X. Wu, "Calcium phosphate glass/MgF<sub>2</sub> double layered composite coating for improving the corrosion resistance of magnesium alloy", *J. Alloys Compd.*, Vol. 591, 2014, pp. 34-40.
- [13] T. Kokubo, H. Takadama, How useful is SBF in predicting in vivo bone bioactivity?, *Biomaterials* Vol. 27, 2006, pp. 2907–2915.
- [14] C. Zhang, C. Liu, Y. Ma, "Preparation of compound coating of fluorine conversion layer and calcium phosphate on AZ31 magnesium alloy", *Mater. Res. Innovations*, Vol. 18, No. sup2, 2014, pp. S2-564-S2-569.
- [15] J. Yang, J. Peng, E.A. Nyberg, F.-s. Pan, "Effect of Ca addition on the corrosion behavior of Mg–Al–Mn alloy", *Appl. Surf. Sci.*, Vol. 369, 2016, pp. 92-100.
- [16] S.Z. Khalajabadi, M.R.A. Kadir, S. Izman, R. Ebrahimi-Kahrizangi, "Fabrication, bio-corrosion behavior and mechanical properties of a mg/ha/mgo nanocomposite for biomedical applications", *Mater. Des.*, Vol. 88, 2015, pp. 1223-1233.
- [17] E. Budke, J. Krempel-Hesse, H. Maidhof, H. Schüssler, "Decorative hard coatings with improved corrosion resistance", *Surf. Coat. Technol.*, Vol. 112, No. 1-3, 1999, pp. 108-113.
- [18] Y. Wan, G. Xiong, H. Luo, F. He, Y. Huang, X. Zhou, "Preparation and characterization of a new biomedical magnesium–calcium alloy", *Mater. Des.*, Vol. 29, No. 10, 2008, pp. 2034-2037.
- [19] X. Gu, W. Zheng, Y. Cheng, Y. Zheng, "A study on alkaline heat treated Mg–Ca alloy for the control of the biocorrosion rate", *Acta Biomater.*, Vol. 5, No. 7, 2009, pp. 2790-2799.
- [20] B.-L. Yu, J.-K. Lin, J.-Y. Uan, "Applications of carbonic acid solution for developing conversion coatings on Mg alloy", *Trans. Nonferrous Met. Soc. China*, Vol. 20, No. 7, 2010, pp. 1331-1339.
- [21] X. Gu, N. Li, W. Zhou, Y. Zheng, X. Zhao, Q. Cai, L. Ruan, "Corrosion resistance and surface biocompatibility of a microarc oxidation coating on a Mg–Ca alloy", *Acta Biomater.*, Vol. 7, No. 4, 2011, pp. 1880-1889.
- [22] H.R. Bakhsheshi-Rad, M.H. Idris, M.R.A. Kadir, M. Daroonparvar, "Effect of fluoride treatment on corrosion behavior of Mg–Ca binary alloy for implant application", *Trans. Nonferrous Met. Soc. China*, Vol. 23, No. 3, 2013, pp. 699-710.